Journal of
Ceramic Science
and Technology

J. Ceram. Sci. Tech., 07 [01] 119-126 (2016)
DOI: 10.4416/JCST2015-00048
available online at: http://www.ceramic-science.com

Influence of Sintering Conditions on the Microstructure and Properties of Alumina-Filled Borosilicate Glass

P.F. Araújo[1], L.B. Daros[1], M. Souza[1], D.E. García[1], D. Hotza[*1, 2]

[1]Graduate Program on Materials Science and Engineering (PGMAT)
[2]Department of Chemical Engineering (EQA)
Federal University of Santa Catarina (UFSC), 88040 - 900 Florianópolis, SC, Brazil
received August 26, 2015; received in revised form November 3, 2015; accepted January 8, 2016

Abstract

Alumina-filled borosilicate glass composites (1-*x*) glass + *x*Al_2O_3 (*x* = 0, 5, 10, 15, 20 vol%) were fabricated by means of conventional sintering at 800 and 850 °C and fast firing at temperatures between 850 and 950 °C. The effect of particle size, heating rate and holding time at maximum temperature on phase composition and densification was investigated. The effect of Al_2O_3 addition on microstructure, flexural strength, fracture toughness, electrical conductivity, and thermal expansion coefficient is reported. Al_2O_3 hinders the formation of cristobalite and enhances the mechanical properties of borosilicate glass. Composites containing 10 vol% alumina fabricated by means of conventional sintering exhibited 98 % TD, flexural strength of 175 MPa and fracture toughness of 1.9 MPa·$m^{1/2}$. Crack path and fracture surface observations showed that crack deflection, crack bridging and pull-out by alumina particles were responsible for the increase in fracture toughness. Samples fabricated by means of fast firing exhibited a decrease in flexural strength of ~ 50 % and an increase in fracture toughness of ~ 40 % when compared to conventional sintering. This behaviour could be related to the presence of microcracks originating from β-to-α cristobalite transformation during rapid cooling from the sintering temperature. In conventionally sintered samples, the addition of 5 vol% alumina to borosilicate glass increases hardness from 4.7 to 5.6 GPa, and the dielectric constant from 5.5 to 6.5.

Keywords: Alumina, borosilicate glass, ceramic-filled glasses, fast firing, sintering

I. Introduction

Ceramic-filled glasses (CFG) are composites consisting of a vitreous matrix and a ceramic filler. The combination of the different physical and chemical properties of the matrix and the filler produces a composite exhibiting an increase in mechanical strength, fracture toughness, hardness, and electrical insulation when compared to pure glasses [1–3, 13]. The low sintering temperature of CFG composites represents a cost-effective alternative to bulk ceramics for use as Low-Temperature Co-fired Ceramics (LTCC) substrates in the microelectronic packaging industry [4]. Sintering temperatures of ~ 800 °C enable co-firing with conductors such as gold and copper [5,6], making CFG composites an ideal packaging material.

Borosilicate glasses show higher electrical insulation and a low coefficient of thermal expansion (CTE) when compared to alumina [1, 2], and higher electrical stability when compared to soda-lime glasses [7]. The sintering behaviour of CFG is largely influenced by the degree of crystallization of the glass matrix. Densification prior to crystallization is essential for forming dense ceramic-filled glass composites [8]. During fabrication, thermal cycles at temperatures > 700 °C for borosilicate glasses show the formation of cristobalite [7, 9]. Crystallization results in pore formation and reduced strength owing to the β-to α-cristobalite transformation on cooling from sintering temperature [10]. Al^{+3} ions inhibit the formation of cristobalite [11], and when alumina is used as filler in CFG [2, 6], the combination of borosilicate glass and alumina results in a material with higher thermal stability than pure glass [12].

CFG have been fabricated using different types of borosilicate glass and ceramic fillers, e.g. lead borosilicate glass with alumina [3, 13, 14], soda-borosilicate glass with alumina or Si_3N_4 whiskers [15, 16], borosilicate glass with fibres of SiC [17], C [18], or zirconia [19, 20], and calcium zinc aluminium borosilicate glass with Li_2O particles [21]. The sintering of borosilicate glass (Pyrex®) using alumina particles and platelets as fillers has been reported [7, 9, 11, 22–25], and a summary of experimental results is presented in Table 1. [22–25]

To the best of our knowledge, no publication on alumina-filled borosilicate glass composites has so far addressed the effect of the heating rate on densification, microstructure development and cristobalite formation, as well as the effect of fast firing and volume fraction of alumina particles on mechanical strength and fracture toughness.

The aim of this work is to establish the relationship between processing parameters and microstructure, glass crystallization and bulk density of alumina-filled borosilicate glass composites and investigate the effect of alumina content on fracture strength, fracture toughness, dielectric constant, hardness, and coefficient of thermal expansion of

* Corresponding author: d.hotza@ufsc.br

alumina-filled borosilicate glass composites fabricated by means of conventional and fast sintering.

II. Experimental Procedure

Borosilicate glass powder, D_{50} = 1 to 64 μm, obtained by dry ball milling from commercial glass cullet (Pyrex®, 79 wt% SiO_2, 13 wt% B_2O_3, 4 wt% Na_2O, 2.5 wt% Al_2O_3 + 2.5 wt% other alkaline oxides), and commercial Al_2O_3 powder (Almatis Premium, Germany, 0.3 to 3 μm average particle size), were used to fabricate alumina-filled borosilicate glass composites. Powder mixtures of borosilicate glass containing 0, 5, 10, 15, 20 vol% alumina, and 3 wt% isopropyl alcohol were mixed for 1 h at 100 rpm in a PVC jar using silicone balls (10 mm diameter). Powder compacts of 47 × 5 × 4 mm^3 were obtained by means of uniaxial pressing at 15 MPa. Samples were conventionally sintered in air in an electrical furnace at temperatures of 800 and 850 °C, for less than 15 min at heating rates from 1 to 15 K/min, and fast-fired by introducing the green samples into a pre-heated furnace at 850 to 950 °C, with holding times of 3 and 5 min.

The bulk density of sintered samples was measured in water using the Archimedes' principle, and the relative density calculated based on the theoretical density of the composites, considering glass and alumina density of 2.23 and 3.94 g/cm^3, respectively.

Crystalline phases present in sintered samples at room temperature were identified by means of x-ray diffraction (XRD, Rigaku Desktop Miniflex II, 30 kV, 15mA, CuKα radiation). Scanning electron microscopy (SEM, Hitachi TM3030) was used to investigate the microstructure on polished surfaces chemically etched for 2 min with hydrofluoric acid (2 wt%). The linear coefficient of thermal expansion (CTE) from 25 to 300 °C was measured in air at a heating rate of 7.5 K/min with a push-rod dilatometer (Netzsch, Mod. DIL 402 C). The flexural strength of sintered samples was determined in ten samples in a three-point-bending test (EMIC, Mod. DL 2000) with a span of 42 mm and loading rate of 1 mm/min.

Fracture toughness (K_{IC}) was calculated using the Lawn and Fuller's model (Equation 1), with the Indentation Crack Length (ICL) method, that is a direct measurement of radial cracks produced by means of Vickers indentation [26].

$$K_{IC} = P/c^{3/2} \quad (1)$$

where P is the contact load; c, the crack length, Ψ, the half-angle of the indentor between opposing pyramid edges; and Ψ = 68°.

Hardness was determined in five samples of each composition by means of Vickers indentation using loads of 2, 3 and 4 N. Cracks paths and fracture surfaces were investigated using SEM. Dielectric constant was determined by parallel plate method, using an LCR meter (Agilent E4980A, Keysight) according to the theoretical equation for the capacitance of parallel plates,

$$C = (\varepsilon_0 \varepsilon_r A)/D \quad (2)$$

where ε_r is the dielectric constant of the material; ε_0, 8.854×10^{-12} F·m^{-1} in vacuum; A, the specimen area; and D, the thickness of the specimen.

III. Results and Discussion

(1) Sintering of borosilicate glass compacts

To maximize densification during sintering, the effect of particle size of borosilicate glass, heating rate holding time and sintering temperature on cristobalite formation and density was analysed, and results are shown in Fig. 1 to 3. As shown in Fig. 1, densification increases with increasing heating rate, i.e. a reduction in residence time at high temperature results in an increase in densification. The amount of cristobalite formed decreases with increasing heating rate (see Fig. 2). Reducing the time at high temperature until the maximum temperature is reached reduces the time for nucleation and crystallization and hinders cristobalite formation, favouring densification. When crystallization occurs before full densification, the reduction of viscous flow of the system hinders densification and a porous body is obtained [27]. Powder compacts fabricated using borosilicate glass powder with a particle size of ~ 20 μm (see Fig. 3), at a sintering temperature of 800 °C, holding time of 5 min and heating rate of 15 K/min result in the highest values for relative density. Those parameters were chosen as standard conditions to sinter borosilicate glass-alumina compacts.

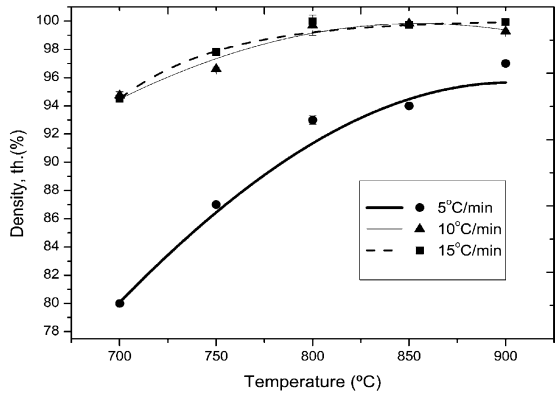

Fig. 1: Relative density of borosilicate glass as a function of the sintering temperature. Holding time 5 min and heating rate as indicated.

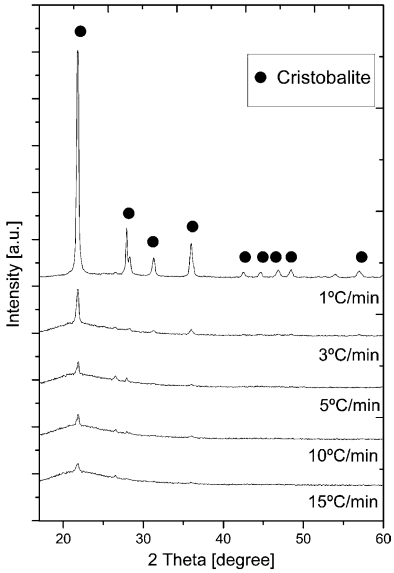

Fig. 2: XRD of borosilicate glass sintered at 800 °C during 5 min. Heating rate as indicated.

Table 1: Experimental data from literature on alumina-filled borosilicate glass composites.

Alumina (vol%)	Morphology	Particle size (μm)	Pressing method	Sintering method	Sintering temperature (°C)	Holding time (min)	Relative density (th%)	Flexural strength (MPa)	Fracture toughness ($MPa \cdot m^{1/2}$)	Dielectric constant (at 1MHz)	CTE ($10^{-6}°C^{-1}$)	Ref.
0 – 10	Particle	0.6	Uniaxial	Conventional	900	240	85	-	-	-	-	[22]
0 – 10	Particle	3	Uniaxial	Conventional	750 – 900	480	-	-	-	-	-	[7]
0 – 30	Platelet	5 – 25	-	Hot pressing	650 – 800	-	99	150	1.9	-	-	[25]
0 – 50	Particle	100	Uniaxial	Conventional	600 – 1000	300	95	-	-	7.2	9.2	[9]
0 – 25	Particle	0.3 – 0.6	Uniaxial	Conventional	950	30	91	-	-	-	-	[23]
0 – 15	Platelet	2 – 5	Uniaxial	Conventional	800	60	97	122	1.4	-	-	[11]
0 – 25	Particle	2.5	Uniaxial	Conventional	800	180	92	-	-	5 – 7.2	5.9	[24]

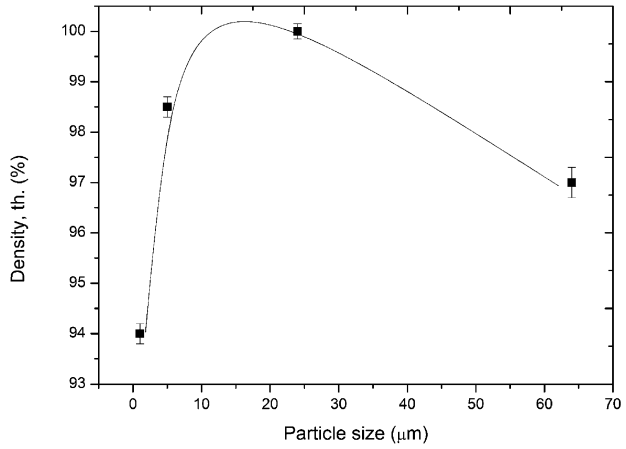

Fig. 3: Relative density of borosilicate glass sintered at 800 °C during 5 min with a heating rate of 15 K/min as a function of the borosilicate glass particle size.

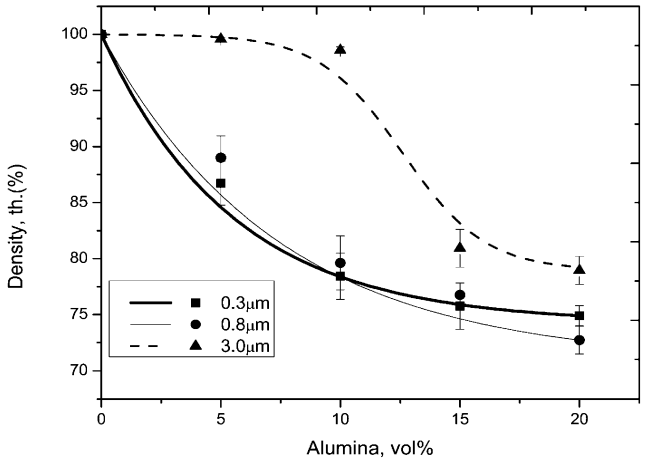

Fig. 4: Relative density of alumina-filled borosilicate glass sintered at 800 °C during 5 min with a heating rate of 15 K/min as a function of the alumina content. Particle size of alumina as indicated.

(2) Conventional sintering of compacts of borosilicate glass and alumina

The effect of the particle size of alumina and its content on the densification of borosilicate glass-alumina compacts was analysed. Samples containing up to 20 vol% alumina and particle size of 0.3, 0.8 and 3 μm were sintered at 800 °C, with corresponding results presented in Fig. 4. The relative density of composites increased with particle size and increasing alumina content. The presence of non-densifying inclusions decreases viscous flow and the effective viscosity of borosilicate glass, reducing densification [28]. Moreover, the presence of rigid inclusions such as alumina in borosilicate glass results in different sintering rates, and the development of transient and residual stresses that hinder densification [29]. Following Bouvard and Lange's model for sphere particles [30], the percolation threshold calculated for alumina with particle size of 0.3, 0.8 and 3 μm was 0.12, 0.15 and 2 vol%, respectively. The alumina content in borosilicate glass is higher than the percolation threshold calculated and therefore the formation of a continuous network of inclusions could be expected which could have reduced the sintering, inhibiting densification [29].

In Fig. 5, for up to 10 vol% alumina, no effect on cristobalite formation has been determined. At higher concentrations, a significant broadening of the main peak of cristobalite was observed at about 22 degrees.

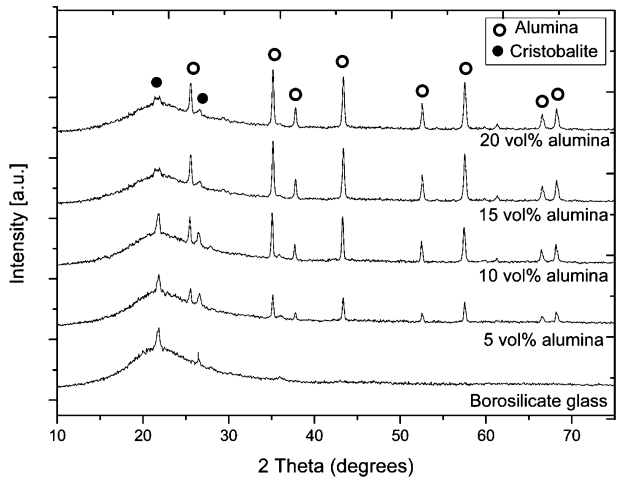

Fig. 5: XRD of alumina-filled borosilicate glass, sintered at 800 °C during 5 min with a heating rate of 15 K/min. Alumina content as indicated.

(3) Fast firing of borosilicate glass and alumina-filled borosilicate glass compacts

As shown in Fig. 1, increasing the heating rate increases densification and hinders crystallization in conventional firing. To investigate the effect on densification and cristobalite formation of the highest heating rate, compacts of borosilicate glass and borosilicate glass containing 5 to 20 vol% alumina were fast-fired by introducing samples into a pre-heated furnace at temperatures between 850 and 1000 °C and holding these for 3 to 5 min; the results are shown in Fig. 6. The highest relative density was obtained after fast firing borosilicate glass compacts for 5 min at 900 °C and 3 min at 950 °C, and for alumina-filled borosilicate glass samples containing 5 vol% alumina after fast firing 5 min at 900 °C. For samples containing > 5 vol% alumina, densification shows similar behaviour to that observed with conventional sintering, which might be related to the same rationale. When compared to conventional sintering, a reduction in sinterability at 850 °C was observed. It is thought that this temperature is not high enough to create a thermal gradient within the compact to favour mass transport during fast firing [31, 32].

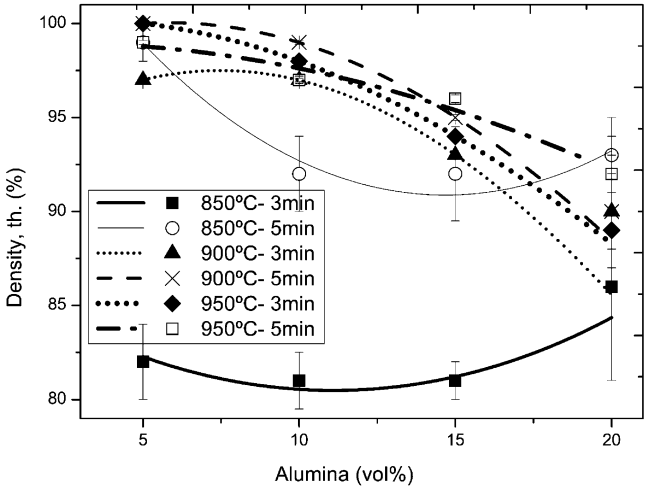

Fig. 6: Relative density of alumina-filled borosilicate glass composites as a function of the alumina content, fast-fired at indicated holding time and temperature.

(4) Flexural strength

(a) *Conventional sintering*

The effect of the addition of alumina particles on flexural strength (σ) of borosilicate glass was investigated, and results showed that an increase in flexural strength of borosilicate glass with alumina addition could be observed from 97 ± 15 MPa for borosilicate glass to 189 ± 32 MPa for composites containing 10 vol% alumina. The increase in σ determined in alumina-filled borosilicate glass composites could be related to load transfer owing to the presence of high-elastic-modulus alumina particles in the glass matrix reducing deformation during loading [33]. On account of the thermal expansion mismatch between borosilicate glass and alumina (3.5 and 9.10^{-6} °C^{-1}), the presence of residual internal compressive stresses in the matrix produced during cooling is expected, and could have further contributed to the increase in strength [25]. The lower amount of cristobalite present in composites on account of alumina addition (see Fig. 5) could have contributed to increasing flexural strength since the detrimental effect related to transformation of β-to α-cristobalite during cooling [9, 10] was reduced.

(b) *Fast firing*

Flexural strength of borosilicate glass and alumina-filled borosilicate glass composites containing 5 and 10 vol% alumina fast-fired at 900 °C for 5 min were determined. The results showed with increasing alumina content, σ increases but when compared to conventionally sintered samples there is a decrease of 55 % in σ for borosilicate glass, 42 and 57 % for composites containing 5 and 10 vol% alumina.

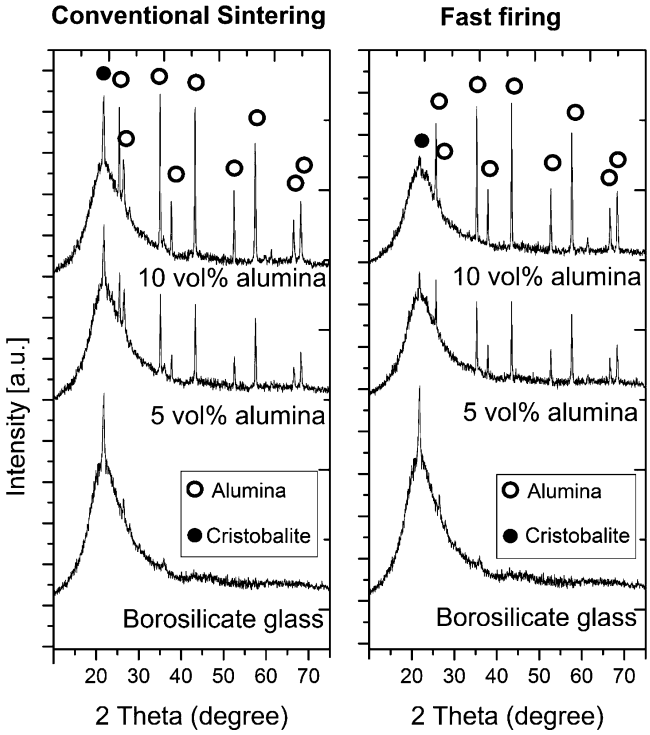

Fig. 7: XRD of samples conventionally sintered at 800 °C during 5 min with a heating rate of 15 K/min and fast fired samples at 900 °C for 5 min.

Based on SEM observations, there was no indication of a change of the defect characteristics of fast-fired samples when compared to conventional sintering. The content of cristobalite formed during fast firing was determined by means of XRD and compared to conventionally sintered samples (see Fig. 7). The amount of cristobalite formed in pure borosilicate glass during conventional sintering and fast firing seems similar. In fast-fired samples the presence of alumina and the short residence time at high temperature hindered crystallization, resulting in peak broadening. It is thought that the decrease in σ could be related to microcrack formation originating from cristobalite transformation on rapid cooling from sintering temperature. The actual transition temperature of cristobalite transformation upon cooling is dependent on the degree of crystallinity of the specimen: well-crystallized materials transform at the highest temperatures; and materials that are

poorly crystallized have lower transition temperatures [34]. As shown in Fig. 7, when compared to conventionally sintered samples, fast-fired samples are less crystalline, so the transformation temperature of cristobalite is expected to be lower than in conventionally sintered samples. As the deformability of borosilicate glass decreases with temperature, i.e. the glass is more rigid, the stress that originated during the β-to α-cristobalite transformation could not be relaxed easily by matrix deformation. Both the rapid cooling and the rigidity of the borosilicate glass could have contributed to avoiding stress relaxation, having as a consequence the formation of microcracks that could have reduced flexural strength.

(5) Fracture toughness

The effect of alumina on fracture toughness (K_{Ic}) of alumina-filled borosilicate glass composites fabricated by means of conventional sintering and fast firing was determined. K_{Ic} increased with increasing alumina content. In conventionally sintered samples K_{Ic} of 0.7 ± 0.1, 1.3 ± 0.1 and 1.9 ± 0.1 MPa·m$^{1/2}$ were measured for borosilicate glass, and composites with 5 and 10 vol% alumina, respectively. In samples sintered in fast firing, K_{Ic} of 1.8, 2.1, and 2.5 were measured for borosilicate glass, and composites with 5 and 10 vol% alumina, respectively. The increase in toughness could be related to crack-tip shielding induced by microcracks [35, 36]. To identify the toughening mechanisms acting upon crack propagation, the crack path of borosilicate glass and composites was analysed by means of SEM (see Fig. 8). In borosilicate glass (Fig. 8a), the crack propagates almost straight. In composites, crack deflection, crack bridging and pull-out were observed as indicated in Fig. 8b, c, d.

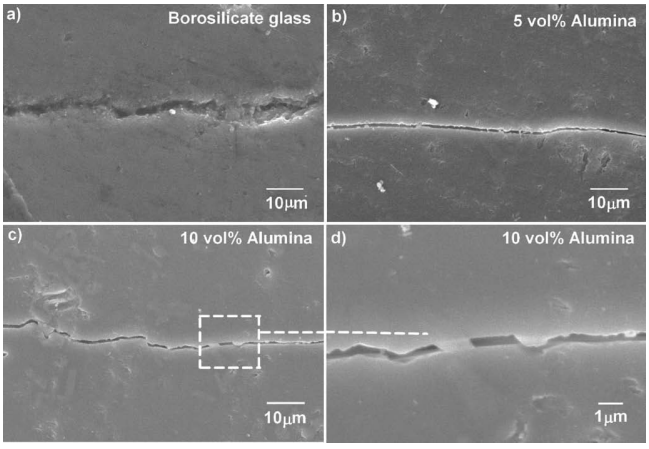

Fig. 8: SEM images of crack path in borosilicate glass and alumina-filled borosilicate glass.

The formation of weak interfaces between alumina grains and borosilicate glass was observed. As shown in Fig. 9, alumina grains seem to detach from borosilicate glass matrix. Owing to the higher CTE of alumina compared to borosilicate glass, a higher shrinkage during cooling is expected, which could have caused the detachment from the matrix. The thermal expansion coefficients mismatch could have also resulted in the formation of radial compressive stresses in the matrix at the particle-matrix interface, the formation of small cracks (see arrows in Fig. 9), leading to the development of weak interfaces that contributed to the observed increase in toughening.

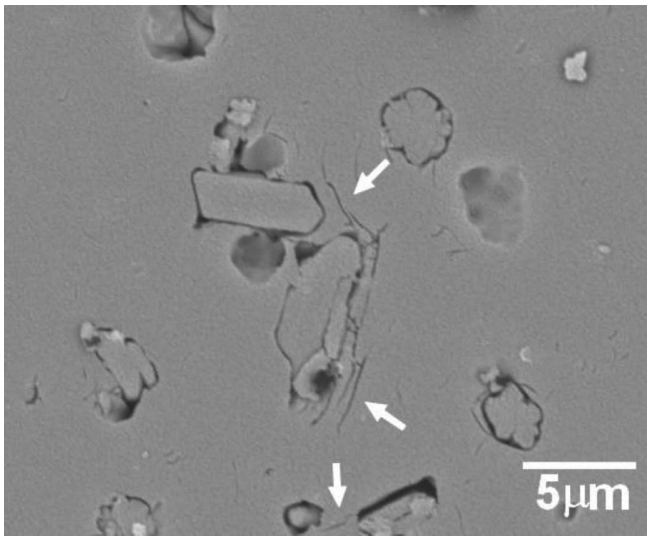

Fig. 9: SEM image of the interface of alumina-borosilicate glass of conventionally sintered alumina-filled borosilicate glass fabricated at 800 °C, sintered for 5 min with a heating rate of 15 K/min.

(6) Hardness, dielectric constant and coefficient of thermal expansion

The effect of alumina on hardness, dielectric constant and coefficient of thermal expansion of borosilicate glass was investigated. Hardness increases with alumina content values of 4.7 ± 0.5, 5.6 ± 0.2 and 4.8 ± 0.3 were determined for conventionally sintered borosilicate glass, and composites with 5 and 10 vol% alumina, respectively, and 3.1 ± 2.2, 4.2 ± 2, 5.1 ± 0.2 for fast-fired samples. Hardness in fast-fired samples decreased when compared to conventionally sintered samples due, possibly, to the formation of microcracks created during rapid cooling as explained previously. In conventionally sintered samples, an increase in the dielectric constant from 5 for borosilicate glass to 7.4 for composites with 10 vol% was determined. The presence of Al^{3+} ions leads to changes in the glass structure, such as substitution of Si^{4+} by Al^{3+}in the glass composition [7, 24]. The substitution of Si^{4+} by Al^{3+} causes an excess of negative charge compensated by the Na^{+} ions contained in the glass network, increasing the number of dipoles, and increasing conductivity [7, 24]. CTE increases with alumina content from $3.5 \cdot 10^{-6}$ °C^{-1} for borosilicate glass to $5.4 \cdot 10^{-6}$ °C^{-1} for alumina-filled borosilicate glass containing 10 % alumina and could be related to the higher CTE of alumina.

IV. Conclusions

Borosilicate glass and alumina-filled borosilicate glass composites were fabricated by means of conventional sintering and fast firing. Increasing the heating rate increases densification and inhibits cristobalite formation in conventionally sintered borosilicate glass. Alumina hinders cristobalite formation in borosilicate glass during conventional sintering, and increases flexural strength and fracture toughness of borosilicate glass. Crack deflection,

crack bridging and pull-out were identified as the toughening mechanisms. Alumina addition increases the hardness, dielectric constant and coefficient of thermal expansion of conventionally sintered borosilicate glass. Alumina addition has no effect on cristobalite formation during fast firing. The flexural strength of the fast-fired borosilicate glass and alumina-filled borosilicate glass composites decreased, and fracture toughness increased, when compared to conventionally sintered samples possibly owing to the presence of microcracks originating from $\beta \rightarrow \alpha$ cristobalite transformation on rapid cooling from the fast-firing temperature.

Acknowledgements

The authors acknowledge CNPq for the financial support.

References

1. Pascual, M.J., Pascual, L., Durán, A.: Modelling of sintering process in borosilicate glasses with rigid inclusions. European Society of Glass Science and Technology, Universite des sciences et techniques du Languedoc; Institut du Verre; International Commission on Glass, in: ESG conference; Glass odyssey 6th, ESG conference, 2002.
2. Kingery, W.D., Bowen, H.K., Uhlmann, D.R.: Introduction to ceramics, 2nd ed. New York: John Wiley & Sons, 1976.
3. Ewsuk, K.G., Harrinson, L.W., Walczak, F.J.: Sintering glass-filled ceramic composites; effects of glass properties. Ceramic Powder Science II, Part B, Ceramic Transactions, edited by Messing, G.L., Fuller, E.R. Westerville, OH: The American Ceramic Society, Inc., **1**, 969 – 977, 1988.
4. Harrison, L.W., Ewsuk, K.G.: Processes for manufacturing tailored property ceramic composites, in design for manufacturability and manufacture of ceramic components, Westerville, OH: The American Ceramic Society, Inc., Ceram. Trans., **49**, 197 – 219, 1995.
5. Ewsuk, K.G., Harrinson, L.W.: Densification of glass-filled alumina composites, in: Sintering of Advanced Ceramics, Ceramic Transactions, edited by Handwerker, C., Blendell, J., Kaysser, W.A., Westerville, OH: The American Ceramic Society, Inc., **7**, 438 – 451, 1990.
6. Park, S.J., Lee, S.J.: Mechanism of preventing crystallization in low-firing glass/ceramic composite substrates, *J. Am. Ceram. Soc.*, **78**, [4], 1128 – 1130, (1995).
7. Jean, J.H., Kuan, T.H.: Crystallization inhibitors during sintering of pyrex borosilicate glass, *J. Mater. Sci. Lett.*, **14**, 1068 – 1070, (1995).
8. Lambrinou, K., Biest, O.V., Boccaccini, A.R., Taplin, D.: Densification and crystallisation behaviour of barium magnesium aluminosilicate glass powder compacts. *J. Eur. Ceram. Soc.*, **16**, [11], 1237 – 1244, (1996).
9. Zawrah, M.F., Hamzawy, E.M.A.: Effect of cristobalite formation on sinterability, microstructure and properties of glass/ceramic composites, *Ceram. Int.*, **28**, 123 – 130, (2002).
10. Holand, W., Beall, G.: Glass-ceramics technology. 1st ed. Westerville, OH: The American Ceramic Society, Inc., 2002.
11. Bernardo, E., Scarinci, G.: Sintering behaviour and mechanical properties of Al_2O_3 platelet-reinforced glass matrix composites obtained by powder technology, *Ceram. Int.*, **30**, 785 – 791, (2004).
12. El-Kheshen, A.A.: Effect of alumina addition on properties of glass/ceramic composite, *Brit. Ceram. Trans.*, **102**, [5], 205 – 209, (2003).
13. Liu, M., Hongqing, Z., Haikui, Z., Zhenxing, Y., Jianxin, Z.: Microstructure and dielectric properties of glass/Al_2O_3 composites with various low softening point borosilicate glasses, *J. Mater. Sci.: Mater. Electron.*, **23**, 2130 – 2139, (2012).
14. Ray, A., Tiwari, A.N.: Compaction and sintering behaviour of glass-alumina composites, *Mater. Chem. Phys.*, **67**, 220 – 225, (2001).
15. Kagawa, Y., Kogo, Y., Hatta, H.: Thermal expansion behavior of the si, N-whisker-reinforced soda-borosilicate glass matrix composite, *J. Am. Ceram. Soc.*, **72**, [6], 1092 – 1094, (1989).
16. Chinnam, R.K., Boccaccini, A.R., Bernardo, E., Epstein, H.: Glass-ceramic composites from borosilicate glass and alumina-rich residues, *J. Appl. Ceram. Tech.*, **12**, [S2], E19 – E27, (2015).
17. Boccaccini, A.R., Janczak-Rusch, J., Pearce, D.H., Kern, H.: Assessment of damage induced by thermal shock in SiC-fiber-reinforced borosilicate glass composites, *Compos. Sci. Technol.*, **59**, 105 – 112, (1999).
18. Klug, T., Bruckner, R.: Preparation of C-fibre borosilicate glass composites: influence of the fibre type on mechanical properties, *J. Mater. Sci.*, **29**, 4013 – 4021, (1994).
19. Duran, A., Pascual, M.J., Pascual, L.: Sintering behaviour of composite materials borosilicate glass-ZrO_2 fibre composite materials, *J. Eur. Ceram. Soc.*, **22**, 1513 – 1524, (2001).
20. Hasanuzzaman, M., Sajjia, M., Rafferty, A., Olabi, A.G.: Thermal behaviour of zircon/zirconia-added chemically durable borosilicate porous glass, *Thermochim. Acta*, **555**, 81 – 88, (2013).
21. Lim, W.B., Saji, V.S., Cho, Y.S., Shul, Y.G., Lim, S., Jang, J.H., Lee, H.R.: Crystallization and dielectric properties of low temperature dielectrics containing Li_2O filler, *J. Non-Cryst. Solids*, **354**, 3849 – 3853, (2008).
22. Jean, J., Gupta, T.K.: Effect of alumina on densification of binary borosilicate glass composite, *J. Mater. Res.*, **9**, [8], 1990 – 1996, (1994).
23. Monteiro, R.C.C., Lima, M.M.R.A.: Effect of compaction on the sintering of borosilicate glass/alumina composites, *J. Eur. Ceram. Soc.*, **23**, 1813 – 1818, (2003).
24. Lima, M.M.R.A., Monteiro, R.C.C., Graça, M.P.F., Ferreira Da Silva, M.G.: Structural, electrical and thermal properties of borosilicate glass-alumina composites. *J. Alloy. Compound.*, **538**, 66 – 2, (2012).
25. Boccaccini, A.R., Trusty, P.A.: Toughening and strengthening of glass by Al_2O_3 platelets, *J. Mater. Sci. Lett.*, **15**, 60 – 63, (1996).
26. Lawn, B.R., Fuller, E.R., Wiederhorn, S.M.: Strength degradation of brittle surfaces: sharp indenters, *J. Am. Ceram. Soc.*, **59**, [5 – 6], 193 – 97, (1976).
27. Lima, M.M., Monteiro, R.: Characterization and thermal behaviour of a borosilicate glass, *Thermochim. Acta*, **373**, 69 – 74, (2001).
28. Boccaccini, A.R.: On the viscosity of glass composites containing rigid inclusions, *J. Mater. Lett.*, **34**, 285 – 289, (1999).
29. Boccaccini, A.R., Olevsky, E.A.: Processing of platelet-reinforced glass matrix composites: effect of inclusions on sintering anisotropy, *J. Mater. Process. Tech.*, **96**, 92 – 101, (1999).
30. Cheng-Hua, K., Gupta, P.K.: Rigidity and conductivity percolation threshold in particulate composites, *Acta Metall. Mater.*, **43**, 397 – 403, (1995).
31. García, D.E., Klein, A.N., Hotza, D.: Advanced ceramics with dense and fine-grained microstructures through fast firing, *Rev. Adv. Mater. Sci.*, **30**, 273 – 281, (2012).
32. Possamai, T.S., Oba, R., Nicolau,V.P., Hotza, D., García, D.E.: Numerical simulation of the fast firing of alumina in a box furnace, *J. Am. Ceram. Soc.*, 95, [12], 3750 – 3757, (2012).
33. Zawrah, M.F.M., El-Kheshen, A.A.: Characterisation of borosilicate glass matrix composites reinforced with SiC or ZrO_2, *Brit. Ceram. Trans.*, **103**, [4], 165 – 170, (2004).

34. Chang-Jun, B.: Integrally cored ceramic investment casting mold fabricated by ceramics, *Int. J. Appl. Ceram. Technol.*, **8**, [6], 1255 – 1262, (2011).

35. Claussen, N., Steeb, J.: Toughening of ceramic composites by oriented nucleation of microcracks, *J. Am. Ceram. Soc.*, **59**, 457 – 458, (1976).

36. Miyata, N., Akada, S., Omura, H., Jinno, H.: Microcrack toughening mechanism in brittle matrix composites. In: Bradt, R.C., Hasselman, D.P.H., Munz, D., Sakai, M., Shevchenko, V. YA. (Ed.). Fracture mechanics of ceramics: Springer US, **9**, [24], 339 – 355, 1992.